BIOCHEMISTRY
including biophysical chemistry & molecular biology
Article

Biochemistry **2009,** *48,* 10005–10013 10005
DOI: 10.1021/bi9014902

Insights into the Molecular Determinants of Proton Inhibition in an Acid-Inactivated Degenerins and Mammalian Epithelial Na^+ Channel†

Ying Wang and Laura Bianchi*

Department of Physiology and Biophysics, Miller School of Medicine, University of Miami, Miami, Florida 33136

Received June 15, 2009; Revised Manuscript Received September 18, 2009

ABSTRACT: Mammalian ASIC channels of the DEG/ENaC superfamily are gated by extracellular protons and function to mediate touch and pain sensitivity, learning and memory, and fear conditioning. The recently solved crystal structure of chicken ASIC1a and preliminary functional studies suggested that a highly negatively charged pocket in the extracellular domain of the channel might be the primary proton binding domain. However, more recent extensive mutagenesis analysis paints a more complex mechanism of channel gating, involving binding of protons at sites immediately after the first transmembrane domain (TM1) and displacement of inhibitory Ca^{2+} ions from the acidic pocket in the extracellular domain and from another Ca^{2+} binding site at the mouth of the pore. We recently identified and functionally characterized *Caenorhabditis elegans* ACD-1, the first acid-inactivated DEG/ENaC channel. ACD-1 is expressed in *C. elegans* amphid glia and functions with neuronal DEG/ENaC channel DEG-1 to mediate acid avoidance and chemotaxis to the amino acid lysine. The post-TM1 residues that were proposed to bind protons in ASIC1a are not conserved in ACD-1, but some of the amino acids constituting the acidic pocket are. However, ACD-1 proton sensitivity is completely independent from extracellular Ca^{2+}, and protons appear to bind the channel in a less cooperative manner. We thus wondered if residues in the acidic pocket might contribute to ACD-1 acid sensitivity. We show here that while ACD-1 sensitivity to extracellular protons is influenced by mutations in the acidic pocket, other sites are likely to participate. We also report that one histidine at the base of the thumb and residues in the channel pore influence proton inhibition in a voltage-independent manner, suggesting that they affect the coupling of proton binding with the gating rather than proton binding itself. We conclude that ACD-1 inhibition by protons is likely mediated by binding of proton ions to multiple sites throughout the extracellular domain of the channel. Our data also support a model in which residues in the acidic pocket contribute to determining the channel state perhaps by changing the strength of the interaction between adjacent thumb and finger domains.

Ion channel subunits of the DEG/ENaC[1] family (named after the *Caenorhabditis elegans* degenerins and the mammalian epithelial Na^+ channels) are two transmembrane domain proteins positioned in the membrane such that short N- and C-termini are located intracellularly while a large loop protrudes extracellularly (*1*, *2*). DEG/ENaC subunits come together in trimers (*3*) to form voltage-independent Na^+ (*1*, *4*) or Na^+ and Ca^{2+} (*5*, *6*) channels, are found across species, and are implicated in an extraordinary range of biological functions including mechanosensation (*7*−*9*), pain sensation (*10*, *11*), thermosensation (*12*), pheromone perception (*13*), proprioception (*14*, *15*), learning and memory (*16*), and Na^+ reabsorption (*1*). In mammals, DEG/ENaC subunits expressed primarily in neuronal tissues are called ASICs (acid-sensing ion channels) and are gated by extracellular protons (*17*). Mammalian epithelially expressed DEG/ENaCs are called ENaCs, are inhibited by intracellular (*18*) but not extracellular protons (*19*), and mediate transport of Na^+ across epithelia (*20*−*22*). We recently reported the characterization of ACD-1, a novel *C. elegans* DEG/ENaC channel. ACD-1 is expressed in *C. elegans* glial amphid sheath cells, is inhibited by both intracellular and extracellular protons, and functions with neuronal DEG/ENaC channel DEG-1 to mediate acid avoidance behavior and chemotaxis to the amino acid lysine (*23*). ACD-1 shares the highest homology with mammalian INaC and BLINaC, two poorly characterized DEG/ENaC subunits expressed in intestine, liver, and brain, and functionally it resembles ENaCs (*24*, *25*).

Recently, the crystal structure of the chicken ASIC1a channel has been solved (*3*). It reveals that ASIC1a subunits resemble a "fist" protruding from the plasma membrane (*3*). The transmembrane domains, posttransmembrane region, and the extracellular domain resemble a forearm, a wrist, and a clenched hand, respectively. A close look at the electrostatic potential mapped onto the solvent-accessible surface reveals the existence of a negatively charged pocket between the "thumb" and the "palm" domains containing three pairs of acidic amino acids that were suggested to coordinate proton binding. Jasti and colleagues indeed demonstrated that mutations of two of these acidic residues (D346 and D350) to asparagine diminish the channel proton sensitivity affecting either the K_i or the cooperativity between protons, or both (*3*). A recent more extensive mutagenesis study, however, has challenged a direct role of the acidic

†This work was supported by American Cancer Society Grant RGS-09-043-01-DDC to L.B. and NIH Training Grant NS07044-33 to Y.W.

*To whom correspondence should be addressed. Phone: 305-243-1887. Fax: 305-243-5931. E-mail: lbianchi@med.miami.edu.

[1]Abbreviations: DEG/ENaC channels, degenerins and the mammalian epithelial Na^+ channels; ASICs, acid-sensitive ion channels; ASIC1a, acid-sensitive ion channel 1a; ACD-1, acid-sensitive channel degenerin-like; INaC, intestinal Na^+ channel; BLINaC, brain, liver, intestine Na^+ channel; TM1, transmembrane domain 1; TM2, transmembrane domain 2; NMDG, *N*-methyl-D-glucamine; BCECF, 2′,7′-bis(carboxyethyl)-5(6)-carboxyfluorescein.

Published on Web 09/21/2009

pocket in proton gating (*26*). Paukert and colleagues found instead that two histidines (H72 and H73) and an aspartic acid (D78) right after transmembrane domain 1 (TM1) are major contributors to the allosteric effect of proton binding that results in gating of the channel. A role of post-TM1 residues in ASIC1a proton gating was previously suggested by the Canessa laboratory (*27*). Paukert and colleagues also reported that residues in the acidic pocket, along with E425 and E432 in the external mouth of the pore, are likely to be involved in binding Ca^{2+}, which exerts an inhibitory effect on ASIC1a stabilizing the closed state (*26*). The authors suggest that protonation of these residues might displace Ca^{2+} favoring channel opening. Another study by Yang and colleagues suggests that the acidic residues of the acidic pocket contribute to stabilize the interaction between the "thumb" and the "finger" domain and that proton binding at these sites may render this interaction stronger, thus triggering channel gating (*28*). The post-TM1 residues that seem to play such a crucial role in proton binding in ASIC1a are not conserved in ACD-1; however, some of the residues in the acidic pocket are. Then again, we show here that ACD-1 pH sensitivity is completely independent from extracellular Ca^{2+}. Thus we reasoned that ACD-1 structural and functional features may shed light onto the mechanism by which the acidic pocket contributes to channel acid sensitivity.

We show here that despite the fact that the pH sensitivity of ACD-1 is independent from extracellular Ca^{2+}, mutations at the acidic pocket influence proton inhibition. We also show that His356 at the base of the "thumb" domain plays a role in proton inhibition and that when mutated to aspartic acid shifts the dose−response curve and reduces the cooperativity between protons in inhibiting the channel. When we simultaneously mutated residues in the acidic pocket and His356, we generated a mutant channel that displayed a pH-insensitive residual current. Since ACD-1 is inhibited rather than activated by protons and its pH sensitivity is Ca^{2+}-independent, our data suggest that the acidic pocket, perhaps via interaction with the finger domain, might be involved in determining whether the open or the close state of the channel is more stable. We also report that mutations in the pore affect proton inhibition in a voltage-independent manner, suggesting that they affect coupling of proton binding to the gating rather than proton binding itself.

MATERIALS AND METHODS

Oocyte Expression, Electrophysiology, and Fluorescence. *acd-1* cDNA was subcloned in the pGEM-HE vector (*23*). Mutations were introduced by PCR using the QuikChange site-directed mutagenesis kit from Stratagene following standard procedures. Capped RNAs were synthesized using the T7 mMESSAGE mMACHINE kit (Ambion), purified (Qiagen RNAeasy columns), and run on denaturating agarose gels to check for size and cRNA integrity. cRNA quantification was then performed spectroscopically. Stage V−VI oocytes were selected among multistaged oocytes dissected by 2 h collagenase treatment (2 mg/mL in Ca^{2+}-free OR2 solution) from *Xenopus laevis* ovaries. Oocytes were incubated in OR2 media, which consists of 82.5 mM NaCl, 2.5 mM KCl, 1 mM $CaCl_2$, 1 mM $MgCl_2$, 1 mM Na_2HPO_4, 0.5 g/L polyvinyl pyrolidone, and 5 mM HEPES (pH 7.2), supplemented with penicillin and streptomycin (0.1 mg/mL) and 2 mM sodium pyruvate. Oocytes were then injected with 69 nL of cRNA mix for a final amount of 5 ng/oocyte of each cRNA. Oocytes were incubated in OR2 plus 500 μM amiloride to inhibit the ACD-1 current and thus prevent Na^+ overload (*29*) at 20 °C for 2−4 days before recording.

Currents were measured using a two-electrode voltage clamp amplifier (GeneClamp 500B; Axon Instruments) at room temperature. Electrodes (0.2−0.5 MΩ) were filled with 3 M KCl, and oocytes were perfused with a NaCl solution containing (in mM) 100 NaCl, 2 KCl, 1 $CaCl_2$, 2 $MgCl_2$, and 10 HEPES. The pH was adjusted at the indicated values using NMDG-Cl or HCl. When we tested solutions at pH lower than 6, we used 10 mM 2-(*N*-morpholino)ethanesulfonic acid (MES) instead of 10 mM HEPES to buffer the solutions. For experiments using 1 mM NaCl the impermeant ion that substituted for Na^+ was $NMDG^+$ (NMDG-Cl, 99 mM). We routinely perfused oocytes with solutions at low pH for only 30 s, which we determined was the time required to fully switch the solution in the recording chamber at our perfusion rate. Chemicals were obtained from Sigma and Calbiochem. We used the pCLAMP suite of programs (Axon Instruments) for data acquisition and analysis. Currents were filtered at 200 Hz and sampled at 1 kHz.

For fluorescence measurements, oocytes were preloaded with 30 μM BCECF for 30 min in OR2 buffer at room temperature (*30*). Fluorescence was measured using a Leica upright microscope equipped with a 20× objective, an Oregon Green filter cube (exciter, HQ495/30X; dichroic, Q515LP; and emitter, HQ545/50m), and a photodiode (pin-020A; UCT Sensors, Inc.) coupled to an Axopatch 200B patch clamp amplifier (Axon Instruments, Inc.). The objective was focused on the animal pole, and fluorescence was monitored with Clampex 8.2 (Axon Instruments, Inc.).

RESULTS

Protons Bind Away from the Ion Permeation Pathway To Inhibit ACD-1 Channel Activity. When we perfuse a *Xenopus* oocyte expressing ACD-1 with a physiological solution at pH 7.2 in which the major carrier ion is Na^+, we detect a large voltage-independent amiloride-sensitive current (*23*). This current resembles currents produced by expression of other DEG/ENaC channels including mammalian ENaCs and *C. elegans* MEC-4(d) and UNC-105(d) (*1*, *29*, *31*) (Figure 1A). If we switch to a solution at pH 5, the current is ~90% inhibited (Figure 1B); return to the solution at pH 7.2 recovers the current to its original level (Figure 1C). Thus, ACD-1 is reversibly inhibited by extracellular acidification (*23*). Since ACD-1 is inhibited by intracellular acidification as well, we confirmed that our manipulations of extracellular pH did not affect intracellular pH using the pH-sensitive fluorescent dye BCECF (*30*). Supporting Information Figure 1 shows that perfusion of extracellular solutions at pH 6.5 and 5.5 for more than 2 min does not result in significant decrease in intracellular pH.

Analysis of the current−voltage relationship at pH 7.2 and 5 indicates that the ACD-1 current is inhibited by protons in a voltage-independent manner (Figure 1D), suggesting that protons do not enter the channel pore. To confirm this, we plotted the pH that gives half-maximal inhibition (K_i) against the voltage (*23*). We found that the K_i does not change with the voltage, supporting the notion that protons do not enter the membrane electric field to inhibit ACD-1 and thus must bind to the extracellular domain of the channel (Figure 1E).

ACD-1 Inhibition by Acidic Solutions Is Independent from Extracellular Ca^{2+} and Na^+. Channels formed by

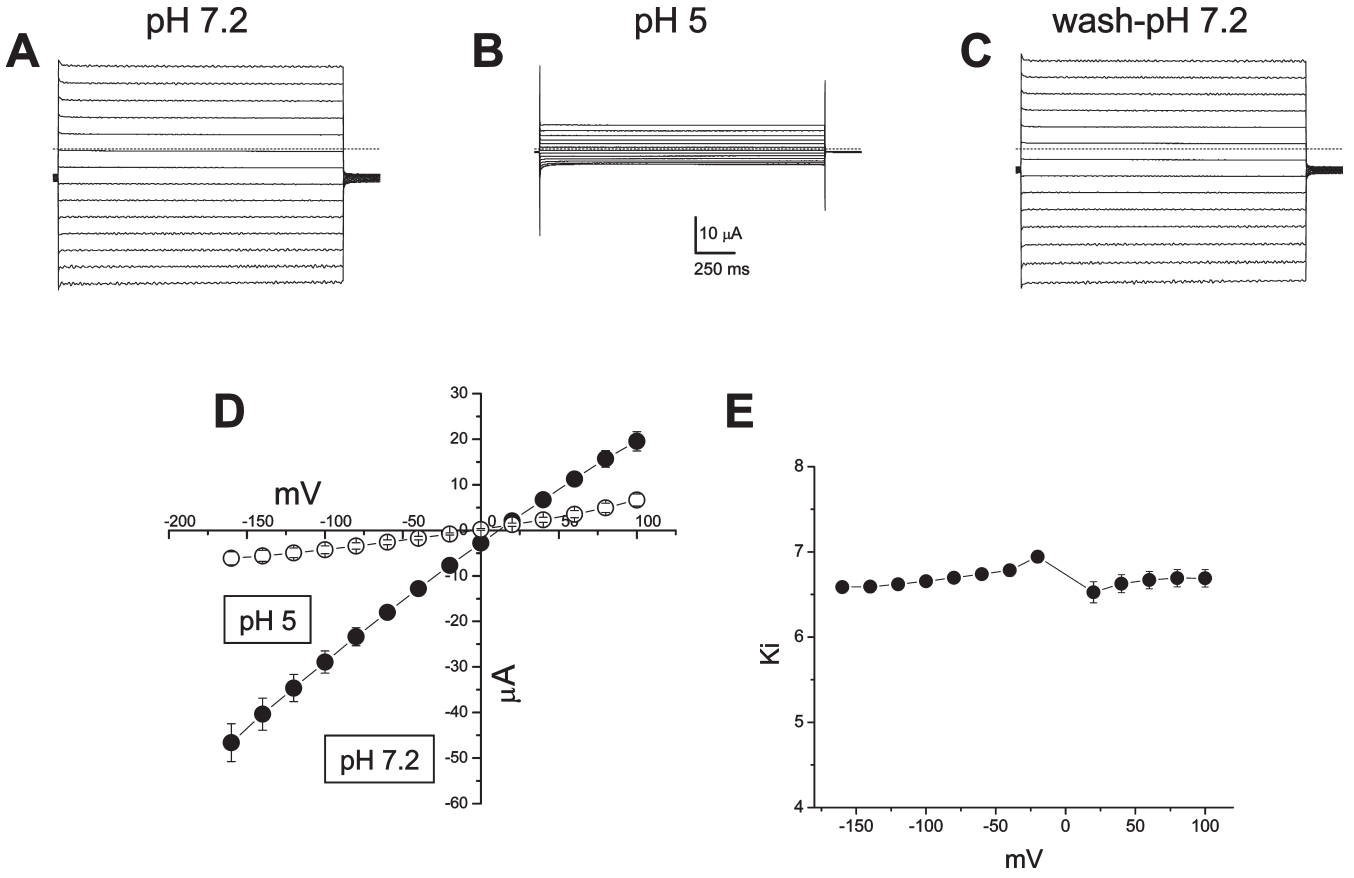

FIGURE 1: ACD-1 currents are reversibly inhibited by application of extracellular acidic solutions. Protons bind away from the ion permeation pathway. (A) Ionic currents recorded in an oocyte injected with *acd-1* cRNA perfused with a physiological NaCl solution. Voltage steps were from −160 to + 100 mV from a holding potential of −30 mV. The same oocyte was perfused with a NaCl solution that was adjusted at pH 5 (B) and was then washed with the solution adjusted at pH 7.2 (C). ACD-1 current is nearly completely inhibited by pH 5 but then recovers to control levels once the oocyte is perfused again with the solution at pH 7.2. The dashed line represents zero current level. (D) Current−voltage relationships of ACD-1 currents measured at pH 7.2 and 5. *n* was 7 in both cases. (E) We plotted the pH that gives half-maximal inhibition (K_i) versus the membrane voltage applied. K_i values were obtained from data reported in ref *23*. The K_i does not change with the voltage, indicating that protons do not enter the membrane electric field to inhibit the channel. $n = 9$. Data are expressed as mean ± SE.

human α, *β*, and *γ* ENaC subunits are potentiated rather than inhibited by extracellular protons (*32*). This potentiating effect is due to protons releasing Na^+ self-inhibition (*32*). Conversely, ASIC channel pH sensitivity is affected by extracellular Ca^{2+} (*33*). We thus wondered if ACD-1 inhibition by protons had anything to do with protons altering the effect of extracellular ions on channel activity. To test this, we first measured ACD-1 acid sensitivity in the absence of Ca^{2+}. When we perfused *Xenopus* oocytes expressing ACD-1 with a solution without $CaCl_2$, we detected an increase in current amplitude, suggesting that Ca^{2+} exerts some type of blocking effect on the ACD-1 channel (Figure 2A), similarly to what we observed for MEC-4(d) and MEC-4(d,G717E) channels (*5*). However, when we determined the pH dose−response curve for ACD-1 currents in the absence of Ca^{2+}, we found that it was identical to the pH dose−response curve determined in extracellular 1 mM $CaCl_2$ (K_i was 6.4 in both cases) (Figure 2B). These results indicate that protons do not interfere with the Ca^{2+} inhibitory effect on ACD-1 channels.

We next tested the effect of Na^+, and measured ACD-1 pH sensitivity in 100 and 1 mM NaCl. Again, dose−response curves were identical in these two conditions, suggesting that Na^+ ions do not interfere with protons (Figure 2B).

The "Acidic Pocket" and Acid Sensitivity. To determine if the *C. elegans* proton-inactivated ACD-1 channel coordinates proton binding using residues corresponding to the ones that were proposed to bind protons in ASIC1a (*3*, *26*), we threaded the ACD-1 sequence onto the chicken ASIC1a crystal structure using the CPHmodels server (http://www.cbs.dtu.dk/services/CPHmodels/). We found that none of the relevant residues in the post-TM1 extracellular domain are conserved in ACD-1 and that, at four of the six positions in which acidic amino acids are found in ASIC1a extracellular acidic pocket, ACD-1 encodes neutral amino acids. However, at position 419 (corresponding to position 346 in chicken ASIC1a) and at position 304 (corresponding to position 238 in chicken ASIC1a) ACD-1 encodes aspartic acids (*3*) (Figure 3A). When we looked at the location of these two acidic residues mapped on the surface of ACD-1, we noted that residues D304 and D419 are in the "palm" and "thumb" domains, respectively, but are next to each other and form an acidic pocket/surface resembling the acidic pocket found in ASIC1a (Figure 3B). To determine if this acidic pocket mediates proton binding in ACD-1, we mutated D419 and D304 to N and assayed channel function. Surprisingly, we found that mutating D419 to N increases rather than decreases ACD-1 proton sensitivity (K_i from 6.4 to 7.3, Figure 3C and ref *23*). By fitting experimental data points with the Hill equation, we found that the *n* coefficient, indicative of cooperativity between protons as they inhibit the channel, decreases from 0.9 to 0.7 in the mutant channel, suggesting increased negative cooperativity between

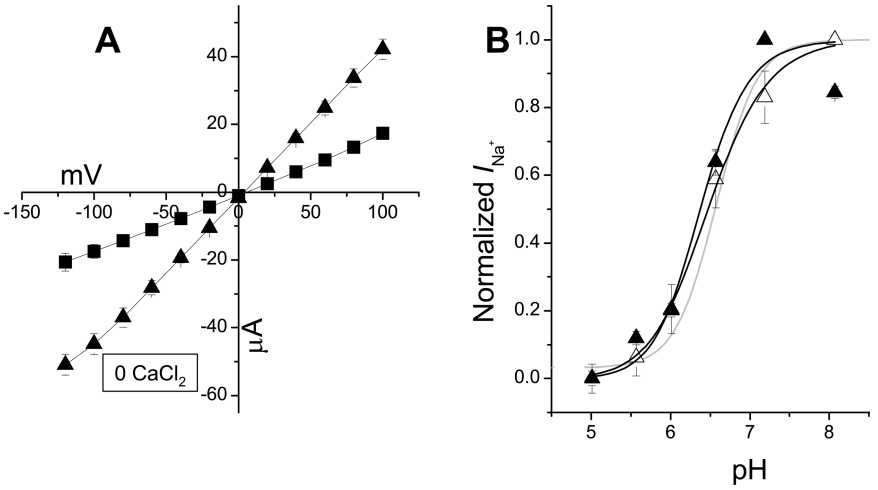

FIGURE 2: Extracellular Ca^{2+} and Na^+ do not interfere with proton inhibition. (A) Current−voltage relationships of ACD-1 currents recorded in physiological saline containing 1 mM $CaCl_2$ (squares) and in 0 mM $CaCl_2$ (triangles) (pH was 7.2 in both cases). ACD-1 current increases upon removal of $CaCl_2$, suggesting that Ca^{2+} inhibits the channel. *n* is 9 each. (B) pH dose−response curves for ACD-1 currents recorded in physiological solution containing 100 mM NaCl + 1 mM $CaCl_2$ (gray curve, from ref *23*), 100 mM NaCl + 0 mM $CaCl_2$ (filled triangles), and 1 mM NaCl + 1 mM $CaCl_2$ (open triangles). All three solutions contained also 2 mM KCl, 2 mM $MgCl_2$, and 10 mM HEPES or MES (see Materials and Methods). Since ACD-1 is impermeable to Ca^{2+} and K^+ ions (*23*), the permeant ion is Na^+ in all cases. Note that the reversal potential of ACD-1 currents was -72 ± 4.2 mV ($n = 13$) in 1 mM NaCl (not shown), predicting an intracellular concentration of Na^+ of ~16 mM. This low concentration of intracellular Na^+ was maintained in oocytes expressing constitutively open ACD-1 channels by our incubation of oocytes in OR2 plus amiloride that prevented Na^+ overload (see Materials and Methods). Data were fitted using the Hill equation. Currents were normalized for the maximal current (usually at pH 7.2 or 8) at −160 mV for all of the pH dose−response curves presented in all of the figures. K_i values were not statistically different, and they were 6.37, 6.45, and 6.47, respectively. *n* is 8 each. Data are expressed as mean ± SE.

protons. Parenthetically, protons bind ASIC1a in a highly cooperative fashion as the *n* coefficient in chicken ASIC1a is 8 (*3*). Our results suggest that mutation D419N may interfere with the interaction between the "thumb" and the "finger" domains perhaps favoring the closed state at higher pHs. However, we cannot exclude the possibility that D419N mutation causes rearrangements of other charges, resulting in increased net negative charges available to protons for binding. We next analyzed ACD-1(D304N) and ACD-1(D304N,D419N). We found that while the ACD-1(D304N) channel is inhibited by acidic solutions similarly to wild type, the double mutant channel has a reduced sensitivity to protons (Figure 3C). Because D304N has unaltered acid sensitivity, it is possible that D419 interacts with another residue in the "palm" domain (based on the crystal structure candidates are not immediately apparent). However, our analysis of the double mutant channel suggests a role for both residues in channel acid sensitivity. We conclude that the acidic pocket formed by residues D304 and D419 participates to proton inhibition but that other sites are likely involved since the ACD-1 double mutant channel is still sensitive to acidic solutions.

Interestingly, when we analyzed the voltage dependence of proton block in ACD-1(D304N), we found that while its proton sensitivity is like wild type at negative voltages, it increases as the voltage becomes more positive (Figure 3D). Since amino acid 304 is not predicted to be in the ion permeation pathway and proton sensitivity increases with depolarization rather than with hyperpolarization, this result suggests that mutations at this site may cause novel residues to move or unmask residues moving out the membrane electric field as the membrane potential becomes more positive. This result thus suggests that at least some of the residues involved in ACD-1 acid inhibition may be located close to the plasma membrane.

Lastly, we wondered if other acidic residues in the "thumb" domain, postulated to play a major role in ASIC1a gating (*3*, *34*), may participate to conferring acid sensitivity to ACD-1. We focused on E428 and E433 because they are the only other two acidic residues that form a clear acidic surface in the "thumb" domain of ACD-1. It is noteworthy however that these two acidic residues are within the "thumb" domain and not between the "thumb" and the "finger" domains. We found that the ACD-1(E428N,E433N) double mutant channels are inhibited by protons just like wild type (Supporting Information Figure 2), suggesting that they do not play any role in ACD-1 acid sensitivity.

A Histidine at the Base of the "Thumb" Influences ACD-1 Acid Sensitivity. Our results suggested that residues close to the plasma membrane may be implicated in ACD-1 inhibition by protons. On the basis of the ASIC1a crystal structure, Jasti and colleagues (*3*) proposed a mechanism of proton-regulated channel gating involving residues at the interface with the plasma membrane. They proposed that Trp 288 in the "thumb" acts like a ball sitting in a socket of the transmembrane domain. They suggested that this residue may couple the movement of the "thumb" caused by protons binding onto the extracellular domain to the movement of the transmembrane domain ultimately resulting in gating. Recent data from the Canessa laboratory confirm this prediction (*34*). When we looked at the ACD-1 sequence, we noticed that ACD-1 also encodes a tryptophan at this site. A histidine (His 356), a residue that can be protonated, is two residues upstream of this tryptophan, and thus it is predicted to be at the interface with the plasma membrane (Figure 4A). We thus wondered if this histidine may be involved in proton binding or in coupling of proton binding to channel gating.

We mutated His 356 to the neutral amino acid alanine, to the negatively charged amino acid aspartate, and to the positively charged arginine. We found that that introduction of a negative charge at this site had a profound effect on the apparent Hill coefficient *n* and a small effect on the K_i, while elimination of a potential protonation site and introduction of a "permanent"

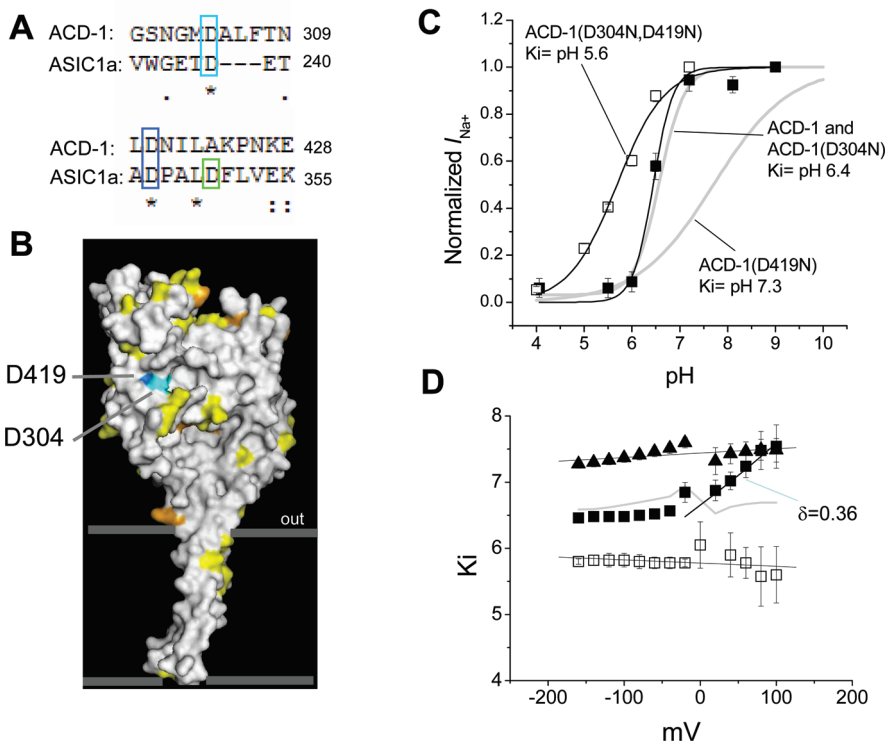

FIGURE 3: Properties of mutants in the "acidic pocket". (A) ACD-1/ASIC1a amino acid alignments highlight the only two conserved acidic residues in the ACD-1 "acidic pocket". D304 corresponds to D238 in chicken ASIC1a, and D419 corresponds to D346 (blue boxes). Chicken ASIC1a has four other acidic residues including D350 (green box) that form with the D238 and D346 negatively charged pocket on the surface the protein. (B) The surface of one ACD-1 channel subunit threaded onto the chicken ASIC1a structure is shown here (*3*). The other two subunits were removed for clarity, and they would be to the right of the one shown. Acidic residues throughout the protein are shown in yellow, histidines are shown in orange, and the two conserved acidic residues D304 and D419 are shown in cyan. (C) pH dose−response curves for wild-type ACD-1, ACD-1(D304N), ACD-1(D419N), and ACD-1(D304N,D419N). Wild-type ACD-1 and ACD-1(D419N) dose−response curves were already reported in ref *23*. Data were fitted using the Hill equation, K_i are shown on the graph, n was ~1 except for ACD-1(D419N) and ACD-1(D304N, D419N), in which it was 0.7. n is 5 each. Average current ratios at pH 6.5 and lower were statistically different by t-test ($p < 0.01$) between ACD-1(D304N,D419N) and wild type or ACD-1(D304N). (D) Voltage dependence of the pH that gives half-maximal inhibition (K_i) for wild-type ACD-1 (gray line), ACD-1(D304N) (filled squares), ACD-1(D419N) (triangles), and ACD-1(D304N,D419N) (open squares). Note that the K_i becomes voltage-dependent at positive voltages in ACD-1(D304N), suggesting that this mutation induces a conformational change in the channel that exposes residues involved in proton binding at more positive potentials. Fit was by linear regression, except for ACD-1(D304N) for which we used the Woodhull equation for voltages between +20 and +100 mV (*48*). Data are expressed as mean ± SE.

positive charge had no effect on channel function or acid inhibition (Figure 4B). This result suggests that protonation of His 356 is not needed for channel inhibition by protons. This result does not support our initial prediction; however, our data suggest a role for this residue in channel inhibition since a negatively charged residue at this site interferes with ACD-1 acid sensitivity.

Since we observed the strongest effect on sensitivity to protons in ACD-1(D304N,D419N) and ACD-1(H356D) mutant channels, we decided to introduce all three mutations in ACD-1 at once to analyze the channel sensitivity to acidic solutions. Interestingly, we found that while the K_i of the triple mutant is similar to the K_i of the double mutant (pH 5.7 for the triple mutant and pH 5.6 for the D304/D419N double mutant), the negative cooperativity between protons in exerting their inhibitory effect on the channel is increased in the triple mutant (n is 0.45 in the triple mutant and 0.7 in the D304/D419N double mutant). In fact, the Hill coefficient of the triple mutant is similar to the Hill coefficient of H356D (n is 0.5). Another difference we noticed is that while pH 4 is sufficient to fully inhibit all of the other mutants we studied, pH 3.5 does not completely inhibit the triple mutant channel: at pH 3.5 14% of the ACD-1(D304N, H356D,D419N) current is still present (Figure 4B). We could not test lower pHs because they affected the oocytes' health and endogenous current; however, the fact that at pH 4 the effect appears saturated suggests that a portion of the current in the ACD-1 triple mutant is pH insensitive. Interestingly, this residual pH-insensitive current was not observed in the double mutant or H356D, suggesting that the effect of these three combined mutations is not additive but rather synergistic.

Contribution of the Second Transmembrane Domain to Acid Inhibition. Residues in the second transmembrane domain (TM2) of DEG/ENaCs have been implicated in controlling channel gating and ion selectivity (*2*, *29*, *35*−*41*). Yang and colleagues have shown that mutations at specific residues within TM2 result in nonfunctional ASIC1a channels, suggesting that they may interfere with proton gating; however, other explanations for lack of channel activity may exist (*28*). ACD-1 is inhibited rather than opened by protons; we thus reasoned that this feature may help to shed light on the role of TM2 residues on proton gating, because lack or reduced effect of protons should not result in nonfunctional ACD-1 channels. We focused on three residues: (1) S513, corresponding to alanine 713 in MEC-4 (the (d) mutation), that when mutated to bulkier residues including Val or Thr hyperactivates the MEC-4 channel (*2*, *31*, *37*, *39*, *42*); (2) G516, that forms a kink in ASIC1a TM2 that constricts the ion permeation pathway (*3*) and that when mutated to glutamic acid in MEC-4 introduces a binding site for extracellular Ca^{2+} (*5*), and (3) I530, that participates to

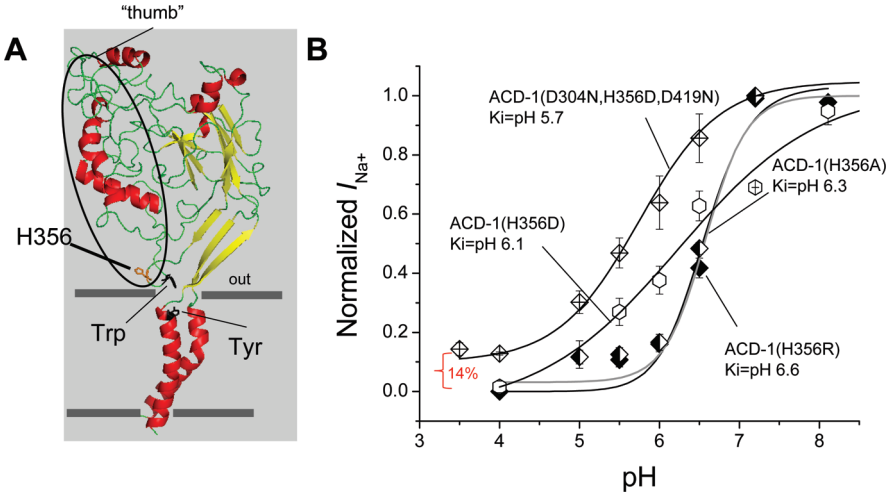

FIGURE 4: Role of a histidine at the base of the "thumb" in proton sensitivity. (A) Secondary and tertiary structure organization of one ACD-1 subunit: α-helices are in red, β-sheets in yellow, and turns in green (PyMol). The ellipse highlights the thumb domain. At the base of the thumb histidine 356 sticks out facing away from the ion permeation pathway. A tryptophan in the thumb domain and a tyrosine in the first transmembrane domain are thought to form $\pi-\pi$ interaction that stabilizes the subunit structure and is crucial for proton-activated gating in ASIC1a (*34*). These two residues are present in ACD-1 as well (in black) although slightly shifted. (B) pH dose−response curves for ACD-1 histidine mutants and the D304N/H356D/D419N triple mutant. Data points were fitted using the Hill equation. K_i values are shown on the graph. The gray line represents the fit for wild-type ACD-1. Note that at pH 3.5 14% of the current carried by the triple mutant channel is still present. We confirmed this by applying 500 μM amiloride, which completely suppressed the current. *n* is 5−10. Data are expressed as mean ± SE. Statistical analysis by *t*-test confirms that current ratios of ACD-1(H356D) and ACD-1(D304N,H356D,D419N) are statistically different from wild type ($p < 0.01$); wild-type values were obtained from ref *23*.

conferring acid sensitivity to β ENaC in a channel complex formed by α and β only (*43*) (Figure 5A,B).

We found that introduction of a valine at the (d) site significantly shifts the pH dose−response curve toward more acidic pH (K_i is 5.5 instead of 6.4), indicating that higher proton concentration is needed to close this mutant channel (Figure 5C). It is noteworthy that ACD-1(d) substitution (S513V) does not cause channel hyperactivation as the channel seems to be fully activated in its wild-type form (*23*). A smaller shift toward more acidic pH was observed for the G516E mutant, suggesting that this residue is also part of the proton gate (Figure 5B). Interestingly, we did not observe activation of the *Xenopus* oocyte endogenous Ca^{2+}-activated Cl^- current, that we used in the past as a measure of MEC-4(d) Ca^{2+} permeability (*5*), when we perfused oocytes expressing ACD-1(G516E) with a $CaCl_2$ solution. These results indicate that this substitution alone does not introduce a Ca^{2+} binding site in ACD-1 (not shown (*5*)). Finally, I530V substitution does not change the pH dose−response curve, suggesting either that other residues in mammalian β ENaC subunits participate with this site to control the gate (*43*) or that the ACD-1 proton gate differs substantially from β ENaC's. Importantly, none of the mutations we engineered introduces voltage dependence to the sensitivity to protons (Figure 5D), indicating that they do not introduce or expose novel proton binding sites in the ion permeation pathway. Rather, these mutations are likely to affect the coupling of the proton binding with the gate. Of note is that all of the mutants we analyzed displayed the same time and voltage independence of WT channels, as well as similar current amplitudes (except for G516E as we report in the paper); they also did not acquire Ca^{2+} permeability (not shown).

DISCUSSION

This study shows that two acidic residues in the extracellular domain and a histidine at the base of the "thumb" domain influence proton gating in the *C. elegans* acid-inactivated DEG/ENaC channel ACD-1. We also report that residues in the second transmembrane domain possibly mediate coupling of proton binding to channel gating and that, contrarily to ASICs and ENaCs, extracellular sodium and calcium do not interfere with proton inhibition of ACD-1.

The Base of the "Thumb" and Channel Gating in the DEG/ENaC Channel Class. The solution of the ASIC1a crystal structure predicted that amino acids at the base of the "thumb" domain would be essential for coupling proton binding to channel gating. Indeed, the base of the thumb is shaped like a tight loop formed by three consecutive prolines, that reaches back toward the plasma membrane almost touching it. It was thus postulated that this loop would interact with the first transmembrane domain of ASIC1a. Specifically, Trp 288 was predicted to form noncovalent interaction with sites in TM1 (*3*, *28*). Recent work from the Canessa laboratory has indeed demonstrated that tryptophan 288 forms noncovalent interaction with tyrosine 72 in TM1 and that such interaction is essential for proton-mediated gating: substitution of either amino acids results in shift of proton sensitivity toward extremely acidic pH essentially resulting in the channel not being gated by testable pHs (below pH 4) (*34*).

ACD-1 encodes a tryptophan at position 358 and a tyrosine at position 127 in TM1, suggesting that the interaction between the base of the thumb domain and TM1 is conserved in *C. elegans* ACD-1 as well. Two residues upstream to Trp 358, histidine 356 sticks out of the protein structure facing away from the central axis of the channel. Our analysis of substitutions at this position suggests that while a potential protonation site is not essential at this position, a negatively charged residue at this site interferes with coupling proton binding to channel inhibition. This interference may be a direct effect on the interaction between Trp 358 and Tyr 72 or an effect mediated by the closely located plasma membrane (for example, through repulsion from the negative surface charges of the plasma membrane). Our results confirm

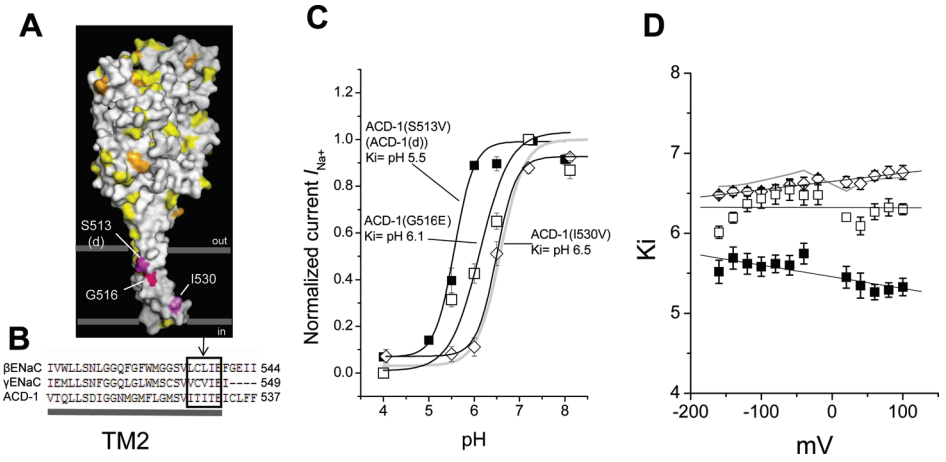

FIGURE 5: Contribution of pore residues to inhibition of ACD-1 by protons. (A) The surface of an ACD-1 subunit is shown here. Yellow and orange are for acidic residues and histidines, respectively. The subunit is rotated ~180° compared to that in Figures 3B and 4A. In purple are the residues that we mutated in the second transmembrane domain and that line the ion permeation pathway. (B) Amino acid alignment of the second transmembrane domain of mammalian β and γ ENaC and *C. elegans* ACD-1. The β ENaC sequence delineated by the box is needed in β/γ chimeras for ENaC channel inhibition by extracellular protons (*43*). (C) pH dose−response curves for ACD-1 pore mutants. Fitting was with the Hill equation. Data are expressed as mean ± SE; statistical analysis by *t*-test ($p < 0.01$) confirms that current ratios of ACD-1(S513V) and ACD-1(G516E) are statistically different from wild type for pH 6.5 and lower. The gray line represents the fit for wild-type ACD-1. K_i values are shown on the graph. *n* is 5−9. (D) Voltage dependence of the pH that gives half-maximal inhibition (K_i) for ACD-1(S513V) ($n = 6$), ACD-1(G516E) ($n = 6$), and ACD-1(I530V) ($n = 5$). In gray is shown the wild-type ACD-1 voltage sensitivity of the proton block. Data are expressed as mean ± SE and were fitted by linear regression.

that the base of the "thumb" domain plays a key role in gating in the channel class.

Residues Lining the Pore Participate in Coupling Proton Binding to Channel Gating. Since the identification of the neurotoxic MEC-4 mutant MEC-4(S713V or T), residues in the second transmembrane domain of DEG/ENaC channels have been implicated in gating (*2*). MEC-4(d) channels are hyperactivated with channel open probability increasing from less than 0.05 in wild-type MEC-4 to 0.5 in MEC-4(d) (*42*), resulting in larger whole cell currents (*29*). MEC-4, which mediates gentle touch sensation in *C. elegans* (*7*), induces neurodegeneration when it becomes hyperactivated (*2*) probably as a result of Na^+/Ca^{2+} overload (*5*). Other members of the DEG/ENaC family including *C. elegans* UNC-105 and mammalian MDEG, hINaC, and BLINaC are hyperactivated by analogous substitutions (*24*, *25*, *31*). We previously reported that introducing a Val at the corresponding residue in ACD-1 (ACD-1(S513V)) does not cause channel hyperactivation (*23*). However, we show here that ACD-1(S513V) channels are less sensitive to extracellular protons. Similarly, G516E substitution shifts the pH dose−response curve toward more acidic pHs. Based on threading of the ACD-1 sequence onto the ASIC1a crystal structure, S513 faces the ion permeation pathway, whereas G516 is facing the inside of the α-helix. It is possible that substituting S513 with a nonpolar residue and G516 with a polar one causes the α-helix to become enough distorted to affect coupling of the proton binding to the gate. In support of this hypothesis we find that ACD-1(G516E) has reduced whole-cell currents (5% of wild-type ACD-1 currents; data not shown). To conclude, we have identified two residues in ACD-1 TM2 that are important for coupling proton binding to channel inhibition. Since in previous work the role of residues in TM2 in coupling of proton binding to gating was inferred based on lack of proton gating and thus activity in TM2 mutants (*26*), we believe that our study provides further and clearer evidence that residues in TM2 couple proton binding to gating.

The Extracellular Domain and Its Influence on Channel Inhibition by Protons. Our work shows that the two conserved acidic residues in ACD-1 (D304 and D419) in the extracellular domain of ACD-1 participate in proton gating. However, our results also suggest that other residues are involved, since neutralization of both charges does not abolish ACD-1 sensitivity to protons. Similarly, Li and colleagues recently showed that neutralization of all the negative charges in the ASIC1a proton sensor does not eliminate ASIC1a sensitivity to protons (*34*). The post-TM1 residues that seem to play a big role in proton gating in ASIC1a possibly binding protons themselves (H72, H73, and D78) are not conserved in ACD-1, excluding the involvement of these residues in ACD-1 acid sensitivity. ACD-1 has 40 negatively charged amino acids and 9 histidines in the extracellular domain, respectively; it will be interesting to determine if a discrete number of these charges bind protons to influence channel function or if the effect of protons is mediated by their interaction with all of these sites. Because residues D304, D419, and H356 are located far away from the channel gate, our results and work from other laboratories draw a picture of a highly dynamic extracellular domain of DEG/ENaC channels when they interact with their ligands (*3*, *28*, *34*, *44*).

Our previous work on homologous *C. elegans* channel MEC-4 had also suggested that large conformational changes occur in the extracellular/transmembrane domain of the channel during gating (*44*). We indeed showed that mutation A149V in the MEC-4 palm domain causes hyperactivation of channels when combined with MEC-10(d), while MEC-10(d), MEC-4(A149V), and MEC-10(d)/MEC-4 channels are not hyperactivated. These data suggest that changes of the extracellular domain structure can have profound effects on how residues located in the transmembrane domain affect gating.

ACD-1 Structure/Function and Implications for Its Role in C. elegans Sensory Perception. ACD-1 is expressed in *C. elegans* amphid sheath cells where it functions to coordinate acid avoidance behavior and chemotaxis to lysine acetate (*23*). Because ACD-1 is sensitive to both extracellular and intracellular acidification and acid avoidance and chemotaxis to lysine acetate are expected to cause extracellular and intracellular acidification,

respectively, we previously proposed a direct link between ACD-1 acid sensitivity and *C. elegans* behavior. In support of our model are our data showing that a higher percentage of *C. elegans deg-1;acd-1* double mutant animals expressing ACD-1(D419N) escape acidic environments as compared to wild animals or *deg-1; acd-1* mutants expressing wild-type ACD-1 (*23*). However, the pH that causes half-maximal inhibition of ACD-1 currents in *Xenopus* oocytes and that induces escape behavior in 50% of the animals does not match (pH 6.4 versus pH 4 (*23*)).

So, why is the ACD-1 channel reconstituted in *Xenopus* oocytes more sensitive to acidic solutions than animals are? One possibility is that other DEG/ENaC channels may be expressed in amphid glia and may form with ACD-1 hetero-multimeric channels with lower pH sensitivity than homomeric ACD-1 channels. This scenario would not be unprecedented since other DEG/ENaC channels have been shown to have different pH sensitivity depending on whether they are assayed in expression systems or in native tissue (see supplementary table in ref *45*). Another possibility is that *C. elegans* endogenous accessory subunits tune ACD-1 acid sensitivity to more acidic pHs *in vivo*. For example, the stomatin-like protein MEC-2 interacts with the transmembrane domains of MEC-4 affecting the permeability properties and activity of the channel (*29*), and the paraoxonase-like protein MEC-6 enhances MEC-4 channel activity by direct binding to MEC-4 (*46*). MEC-2 and MEC-6 do not change ACD-1 properties in *Xenopus* oocytes (not shown) and are not expected to be expressed in amphid glia (*46*, *47*); however, seven other stomatin-like proteins are encoded by the *C. elegans* genome, and their expression pattern and function are currently unknown. Our structure/function analysis suggests that accessory or other DEG/ENaC subunits that interact with residues D304, H356, D419, S513, and G516 may have profound effects on ACD-1 pH sensitivity.

ACKNOWLEDGMENT

We thank the Dahl laboratory for providing *X. laevis* oocytes and Peter Larsson for critical reading of the manuscript and for help with the fluorescent experiments.

SUPPORTING INFORMATION AVAILABLE

Two figures showing no effect of extracellular acidic solutions on intracellular pH in *Xenopus* oocytes and no participation of E428 and E433 residues to ACD-1 acid sensitivity. This material is available free of charge via the Internet at http://pubs.acs.org.

REFERENCES

1. Canessa, C. M., Horisberger, J. D., and Rossier, B. C. (1993) Epithelial sodium channel related to proteins involved in neurodegeneration. *Nature 361*, 467–470.
2. Driscoll, M., and Chalfie, M. (1991) The *mec-4* gene is a member of a family of *Caenorhabditis elegans* genes that can mutate to induce neuronal degeneration. *Nature 349*, 588–593.
3. Jasti, J., Furukawa, H., Gonzales, E. B., and Gouaux, E. (2007) Structure of acid-sensing ion channel 1 at 1.9 Å resolution and low pH. *Nature 449*, 316–323.
4. Canessa, C. M., Schild, L., Buell, G., Thorens, B., Gautschi, I., Horisberger, J. D., and Rossier, B. C. (1994) Amiloride-sensitive epithelial Na^+ channel is made of three homologous subunits. *Nature 367*, 412–413.
5. Bianchi, L., Gerstbrein, B., Frokjaer-Jensen, C., Royal, D. C., Mukherjee, G., Royal, M. A., Xue, J., Schafer, W. R., and Driscoll, M. (2004) The neurotoxic MEC-4(d) DEG/ENaC sodium channel conducts calcium: implications for necrosis initiation. *Nat. Neurosci. 7*, 1337–1344.
6. Xiong, Z. G., Zhu, X. M., Chu, X. P., Minami, M., Hey, J., Wei, W. L., MacDonald, J. F., Wemmie, J. A., Price, M. P., Welsh, M. J., and Simon, R. P. (2004) Neuroprotection in ischemia: blocking calcium-permeable acid-sensing ion channels. *Cell 118*, 687–698.
7. Chalfie, M., and Sulston, J. (1981) Developmental genetics of the mechanosensory neurons of *Caenorhabditis elegans*. *Dev. Biol. 82*, 358–370.
8. Price, M. P., Lewin, G. R., McIlwrath, S. L., Cheng, C., Xie, J., Heppenstall, P. A., Stucky, C. L., Mannsfeldt, A. G., Brennan, T. J., Drummond, H. A., Qiao, J., Benson, C. J., Tarr, D. E., Hrstka, R. F., Yang, B., Williamson, R. A., and Welsh, M. J. (2000) The mammalian sodium channel BNC1 is required for normal touch sensation. *Nature 407*, 1007–1011.
9. Price, M. P., McIlwrath, S. L., Xie, J., Cheng, C., Qiao, J., Tarr, D. E., Sluka, K. A., Brennan, T. J., Lewin, G. R., and Welsh, M. J. (2001) The DRASIC cation channel contributes to the detection of cutaneous touch and acid stimuli in mice. *Neuron 32*, 1071–1083.
10. Chen, C. C., Zimmer, A., Sun, W. H., Hall, J., and Brownstein, M. J. (2002) A role for ASIC3 in the modulation of high-intensity pain stimuli. *Proc. Natl. Acad. Sci. U.S.A. 99*, 8992–8997.
11. Sluka, K. A., Price, M. P., Breese, N. M., Stucky, C. L., Wemmie, J. A., and Welsh, M. J. (2003) Chronic hyperalgesia induced by repeated acid injections in muscle is abolished by the loss of ASIC3, but not ASIC1. *Pain 106*, 229–239.
12. Askwith, C. C., Benson, C. J., Welsh, M. J., and Snyder, P. M. (2001) DEG/ENaC ion channels involved in sensory transduction are modulated by cold temperature. *Proc. Natl. Acad. Sci. U.S.A. 98*, 6459–6463.
13. Lin, H., Mann, K. J., Starostina, E., Kinser, R. D., and Pikielny, C. W. (2005) A *Drosophila* DEG/ENaC channel subunit is required for male response to female pheromones. *Proc. Natl. Acad. Sci. U.S.A. 102*, 12831–12836.
14. Shreffler, W., Magardino, T., Shekdar, K., and Wolinsky, E. (1995) The unc-8 and sup-40 genes regulate ion channel function in *Caenorhabditis elegans* motorneurons. *Genetics 139*, 1261–1272.
15. Tavernarakis, N., Shreffler, W., Wang, S., and Driscoll, M. (1997) *unc-8*, a DEG/ENaC family member, encodes a subunit of a candidate mechanically gated channel that modulates *C. elegans* locomotion. *Neuron 18*, 107–119.
16. Wemmie, J. A., Chen, J., Askwith, C. C., Hruska-Hageman, A. M., Price, M. P., Nolan, B. C., Yoder, P. G., Lamani, E., Hoshi, T., John, H., Freeman, J., and Welsh, M. J. (2002) The acid-activated ion channel ASIC contributes to synaptic plasticity, learning and memory. *Neuron 34*, 463–477.
17. Krishtal, O. (2003) The ASICs: signaling molecules? Modulators? *Trends Neurosci 26*, 477–483.
18. Garty, H., Asher, C., and Yeger, O. (1987) Direct inhibition of epithelial Na^+ channels by a pH-dependent interaction with calcium, and by other divalent ions. *J. Membr. Biol. 95*, 151–162.
19. Awayda, M. S., Boudreaux, M. J., Reger, R. L., and Hamm, L. L. (2000) Regulation of the epithelial Na(+) channel by extracellular acidification. *Am. J. Physiol. Cell Physiol. 279*, C1896–C1905.
20. Barker, P. M., Nguyen, M. S., Gatzy, J. T., Grubb, B., Norman, H., Hummler, E., Rossier, B., Boucher, R. C., and Koller, B. (1998) Role of gammaENaC subunit in lung liquid clearance and electrolyte balance in newborn mice. Insights into perinatal adaptation and pseudohypoaldosteronism. *J. Clin. Invest. 102*, 1634–1640.
21. Hummler, E., Barker, P., Gatzy, J., Beermann, F., Verdumo, C., Schmidt, A., Boucher, R., and Rossier, B. C. (1996) Early death due to defective neonatal lung liquid clearance in alpha-ENaC-deficient mice. *Nat. Genet. 12*, 325–328.
22. Garty, H., and Palmer, L. G. (1997) Epithelial sodium channels: function, structure, and regulation. *Physiol. Rev. 77*, 359–396.
23. Wang, Y., Apicella, A. Jr., Lee, S. K., Ezcurra, M., Slone, R. D., Goldmit, M., Schafer, W. R., Shaham, S., Driscoll, M., and Bianchi, L. (2008) A glial DEG/ENaC channel functions with neuronal channel DEG-1 to mediate specific sensory functions in C. elegans. *EMBO J. 27*, 2388–2399.
24. Sakai, H., Lingueglia, E., Champigny, G., Mattei, M. G., and Lazdunski, M. (1999) Cloning and functional expression of a novel degenerin-like Na^+ channel gene in mammals. *J. Physiol. 519* (Part 2), 323–333.
25. Schaefer, L., Sakai, H., Mattei, M., Lazdunski, M., and Lingueglia, E. (2000) Molecular cloning, functional expression and chromosomal localization of an amiloride-sensitive Na(+) channel from human small intestine. *FEBS Lett. 471*, 205–210.
26. Paukert, M., Chen, X., Polleichtner, G., Schindelin, H., and Grunder, S. (2008) Candidate amino acids involved in H^+ gating of acid-sensing ion channel 1a. *J. Biol. Chem. 283*, 572–581.

27. Coric, T., Zheng, D., Gerstein, M., and Canessa, C. M. (2005) Proton sensitivity of ASIC1 appeared with the rise of fishes by changes of residues in the region that follows TM1 in the ectodomain of the channel. *J. Physiol. 568*, 725–735.
28. Yang, H., Yu, Y., Li, W. G., Yu, F., Cao, H., Xu, T. L., and Jiang, H. (2009) Inherent dynamics of the acid-sensing ion channel 1 correlates with the gating mechanism. *PLoS Biol. 7*, 13.
29. Goodman, M. B., Ernstrom, G. G., Chelur, D. S., O'Hagan, R., Yao, C. A., and Chalfie, M. (2002) MEC-2 regulates C. elegans DEG/ENaC channels needed for mechanosensation. *Nature 415*, 1039–1042.
30. Ortiz, D., Sanchez, M. A., Koch, H. P., Larsson, H. P., and Landfear, S. M. (2009) An acid-activated nucleobase transporter from *Leishmania major*. *J. Biol. Chem. 284*, 16164–16169.
31. Garcia-Anoveros, J., Garcia, J. A., Liu, J. D., and Corey, D. P. (1998) The nematode degenerin UNC-105 forms ion channels that are activated by degeneration- or hypercontraction-causing mutations. *Neuron 20*, 1231–1241.
32. Collier, D. M., and Snyder, P. M. (2008) Extracellular protons regulate human ENaC by modulating Na^+ self-inhibition. *J. Biol. Chem. 284*, 792–798.
33. Paukert, M., Babini, E., Pusch, M., and Grunder, S. (2004) Identification of the Ca^{2+} blocking site of acid-sensing ion channel (ASIC) 1: implications for channel gating. *J. Gen. Physiol. 124*, 383–394.
34. Li, T., Yang, Y., and Canessa, C. M. (2009) Interaction of the aromatics Tyr-72/Trp-288 in the interface of the extracellular and transmembrane domains is essential for proton gating of acid-sensing ion channels. *J. Biol. Chem. 284*, 4689–4694.
35. Chalfie, M., and Wolinsky, E. (1990) The identification and suppression of inherited neurodegeneration in *Caenorhabditis elegans*. *Nature 345*, 410–416.
36. Hong, K., and Driscoll, M. (1994) A transmembrane domain of the putative channel subunit MEC-4 influences mechanotransduction and neurodegeneration in *C. elegans*. *Nature 367*, 470–473.
37. Waldmann, R., Champigny, G., Voilley, N., Lauritzen, I., and Lazdunski, M. (1996) The mammalian degenerin MDEG, an amiloride-sensitive cation channel activated by mutations causing neurodegeneration in *Caenorhabditis elegans*. *J. Biol. Chem. 271*, 10433–10436.
38. Schild, L., Schneeberger, E., Gautschi, I., and Firsov, D. (1997) Identification of amino acid residues in the alpha, beta, and gamma subunits of the epithelial sodium channel (ENaC) involved in amiloride block and ion permeation. *J. Gen. Physiol. 109*, 15–26.
39. Adams, C. M., Anderson, M. G., Motto, D. G., Price, M. P., Johnson, W. A., and Welsh, M. J. (1998) Ripped pocket and pickpocket, novel *Drosophila* DEG/ENaC subunits expressed in early development and in mechanosensory neurons. *J. Cell Biol. 140*, 143–152.
40. Kellenberger, S., Gautschi, I., and Schild, L. (1999) A single point mutation in the pore region of the epithelial Na^+ channel changes ion selectivity by modifying molecular sieving. *Proc. Natl. Acad. Sci. U.S.A. 96*, 4170–4175.
41. Kellenberger, S., Auberson, M., Gautschi, I., Schneeberger, E., and Schild, L. (2001) Permeability properties of ENaC selectivity filter mutants. *J. Gen. Physiol. 118*, 679–692.
42. Brown, A. L., Fernandez-Illescas, S. M., Liao, Z., and Goodman, M. B. (2007) Gain-of-function mutations in the MEC-4 DEG/ENaC sensory mechanotransduction channel alter gating and drug blockade. *J. Gen. Physiol. 129*, 161–173.
43. Zhang, P., Fyfe, G. K., Grichtchenko, II, and Canessa, C. M. (1999) Inhibition of alphabeta epithelial sodium channels by external protons indicates that the second hydrophobic domain contains structural elements for closing the pore. *Biophys. J. 77*, 3043–3051.
44. Zhang, W., Bianchi, L., Lee, W. H., Wang, Y., Israel, S., and Driscoll, M. (2008) Intersubunit interactions between mutant DEG/ENaCs induce synthetic neurotoxicity. *Cell Death Differ. 15*, 1794–1803.
45. Bianchi, L., and Driscoll, M. (2002) Protons at the gate: DEG/ENaC ion channels help us feel and remember. *Neuron 34*, 337–340.
46. Chelur, D. S., Ernstrom, G. G., Goodman, M. B., Yao, C. A., Chen, L., O'Hagan, R., and Chalfie, M. (2002) The mechanosensory protein MEC-6 is a subunit of the *C. elegans* touch-cell degenerin channel. *Nature 420*, 669–673.
47. Huang, L. S., and Sternberg, P. W. (1995) Genetic dissection of developmental pathways. *Methods Cell Biol. 48*, 97–122.
48. Woodhull, A. M. (1973) Ionic blockage of sodium channels in nerve. *J. Gen. Physiol. 61*, 687–708.